This is a pre-print version of an article published in **Pulatsu B., Erdogmus E. and Lourenço P.B. (2019) *Discrete-continuum approach to assess 3D failure modes of masonry arch bridges,* IABSE Symposium, March 27-29**.

Discrete-continuum approach to assess 3D failure modes of masonry arch bridges

Bora Pulatsu, Ece Erdogmus

University of Nebraska-Lincoln, United States

Paulo B. Lourenço

University of Minho, Guimarães, Portugal

Contacting author: bpulatsu2@unl.com

Abstract

There are two main objectives of this research. First, a full masonry arch bridge with all structural components are considered. The failure mechanism of spandrel wall and backfill-masonry interaction are successfully simulated using a 3D discrete-continuum model as validated by previously published experimental data. Moreover, the influence of the frictional resistance between soil and masonry components is discussed. Second, two different skew arches, with different bond patterns, are analysed to understand the influence of construction method (helicoidal and false) on the damage pattern and capacity. The results of the analysis demonstrated that discrete and mixed discrete-continuum approaches can predict complex 3D collapse mechanisms of masonry arch bridges and provides detailed information about their damage progression.

Keywords: DEM, Mixed discrete-continuum approach, Skew arch, Spandrel wall collapse.

1. Introduction

Masonry arch bridges constitute a significant amount of transportation facilities in European countries. There is also around 1700 masonry arch bridges in United States, where the majority of them exist in the northeastern part of the country [1]. In addition to their transportation purposes, many bridges have historical significance and their assessment requires utmost attention to maintain their structural integrity. In this context, 2D and 3D numerical modelling strategies have been used to analyse these structures since early 1990s. Additionally, several destructive tests of scaled masonry arch structures (laboratory models) and field tests have been performed [2,3,4]. The results of early studies provided a better understanding of the strength and collapse mechanism of masonry arch bridges [5,6]. Most of these studies, both experimental and numerical, focus on the capacity of the arch barrel in the span direction (in-plane), although, spandrel wall collapses, and transverse deformations are also relevant in terms of the load carrying capacity and the serviceability of the masonry arch bridges.

In this study, to represent the full structural response of a masonry arch bridge, a 3D modelling strategy is applied. It is important to note that the performed numerical analysis should address the plasticity of soil material, backfill-masonry interaction and possible damage progression in the structure, i.e. masonry joint cracks, sliding of masonry units and large deformations of spandrel wall. As a result, a mixed modelling strategy is

applied to take advantage of both continuum and discontinuum approaches, as previously proposed by the authors [7,8]. Mixed discrete-continuum model (MDC) is validated by a large-scale experimental study, which demonstrates the failure of spandrel wall due to internal soil pressure. Then, the validated model is employed for parametric analysis to observe the interaction between backfill material and masonry. Finally, skew arches, constructed by helicoidal and false methods, are investigated under the effect of point and line-load. Their collapse mechanism and load capacities are discussed.

2. Mixed discrete-continuum approach

The composite nature of masonry arch bridges requires advanced numerical tools to simulate their behaviour in detail. Here, a mixed approach is employed in the framework of discontinuum analysis, where masonry units and joints are explicitly represented. The explained numerical modelling technique is performed by using a 3D discrete element modelling software 3DEC, developed by Itasca.

In discrete element method (DEM), discontinuous systems may be represented as a group of rigid and/or deformable blocks. The deformability is provided by subdividing blocks internally into tetrahedral finite element zones that may have linear or non-linear constitutive laws. The complex mechanical interaction between blocks is modeled using point contact hypothesis. In this research, soft-contact approach is used, in which penetration of one block to another is allowed and relative displacement of neighbouring blocks are calculated. Moreover, a contact detection algorithm is utilized to update contact condition through sub-contacts for each block through the dynamic process of numerical analysis [9]. The representation of sub-contacts between two adjacent blocks and assigned contact properties, including normal stiffness (k_s), shear stiffness (k_n) tensile strength (f_t), cohesion (c) and friction angle (ϕ), in two orthogonal directions (2D) is given in Figure 1.

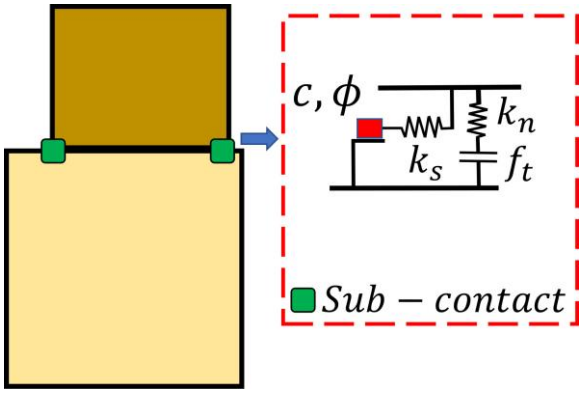

Figure 1. Illustration of sub-contact and contact parameters.

An explicit algorithm is used to solve the equations of motion for the blocks via central difference method. Hence, in each time step, new block positions and displacements are calculated by integrating the law of motion. Then, contact force-displacement law is applied to obtain the new sub-contact forces used in the next time step. The static solutions are obtained by means of dynamic relaxation method and scaled masses are used to improve convergence. The mentioned explicit dynamic solution scheme is repeated until the desired level of convergence is reached.

Throughout this research, DEM is utilized to represent masonry units as distinct rigid blocks and weak planes of masonry joints (unit/mortar interfaces) are simulated as discontinuities. The soil backfill is replicated by a continuum deformable block with a nonlinear plastic constitutive model. Mohr-Coulomb criterion with tension cut-off is used as zone constitutive model for soil backfill. Furthermore, the Coulomb-Slip joint model is used to consider shear and tensile failure modes at the contacts. Both normal and shear contact constitutive behaviours are shown in Figure 2 and Figure 3, respectively.

In shear, cohesion and friction angle reduction at the joints after reaching the shear strength is adjusted defining a residual cohesion (c_{res}) and friction angle (ϕ_{res}). There is no dilatancy set to the joints (non-associative flow).

This is a pre-print version of an article published in **Pulatsu B., Erdogmus E. and Lourenço P.B. (2019)** ***Discrete-continuum approach to assess 3D failure modes of masonry arch bridges,*** **IABSE Symposium, March 27-29**.

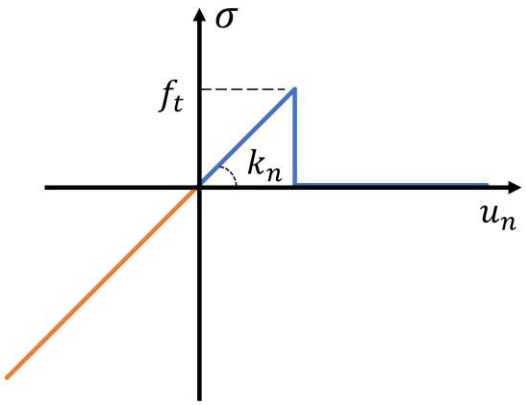

Figure 2. Contact constitutive law in normal direction

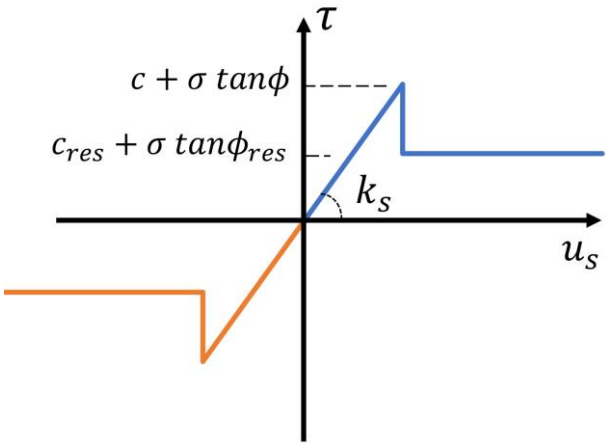

Figure 3. Contact constitutive law in shear direction

It is important to note that the explicit solution procedure of DEM is conditionally stable, hence the time step, Δt, must be kept below the value of critical time step to maintain the numerical stability. The critical time step is calculated as

$$\Delta t_c = (frac)\ 2\left(\frac{M_{min}}{K_{max}}\right)^{0.5} \quad (1)$$

where $frac$, M_{min} and K_{max} are a defined factor, considering that a block may have multiple contact and the default value is 0.1, the minimum mass of an individual block and the maximum contact stiffness in the system, respectively. Thus, calculation cycle of the mentioned explicit solution scheme is given in Figure 4.

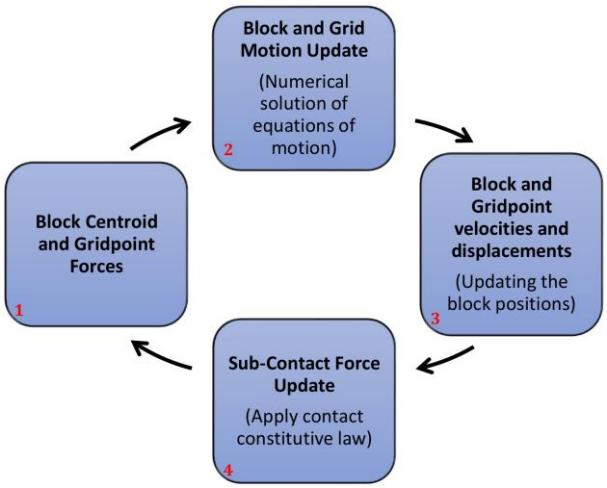

Figure 4. Calculation cycle

3. Out-of-plane failure mode of spandrel walls

The recent inspections of existing masonry arch bridges and laboratory tests indicated the importance of spandrel wall damage for the overall strength and stability of a masonry arch bridge. The arch barrel detachment, out-of-plumbness and collapse state of spandrel walls are noticed by several researchers [10,11]. Thus, to better understand the deformation in the transverse direction and 3D collapse mechanisms, the results of the simulations are benchmarked against previous experimental work on large-scale bridge model [12].

3.1 Experimental setup and model bridge

The model bridge was constructed at the Pennsylvania Transportation Institute Test Track, Pennsylvania in 1996 and tested in 2001 [12]. It is composed of a single span circular arch, spandrel walls, and fill material built by a professional mason. Solid clay bricks and ASTM C270 Type O mortar were used in the construction (Figure 5). The summary of geometrical properties of this large-scale model bridge is given in Table 1.

In Table 2, soil backfill properties are given, which are taken from the relevant studies either in the literature or material characterization tests during the experiment [13].

This is a pre-print version of an article published in **Pulatsu B., Erdogmus E. and Lourenço P.B. (2019)** ***Discrete-continuum approach to assess 3D failure modes of masonry arch bridges,*** **IABSE Symposium, March 27-29**.

Figure 5. Large-scale bridge model

Table 1 Geometrical properties of model bridge

Height [m]	Length [m]	Total width [m]	Clear width of the fill [m]
1.8	4	1.5	1.1
Arch span [m]	**Arch thickness [cm]**	**Height of the fill [m]**	**Intrados radius of arch [m]**
1.5	20	1.675	0.75

Table 2. Soil Backfill Properties

Density [kg/m^3]	Elastic Modulus [MPa]	Cohesion [kPa]	Friction Angle [°]	Poisson's ratio [-]
2200	200	20	38	0.3

The external loads are applied at the quarter span on a loading plate as shown in Figure 6. Transverse displacements are recorded at different locations and the maximum transversal deformation is measured on the top corner of the spandrel wall, which is shown in a red box in Figure 6.

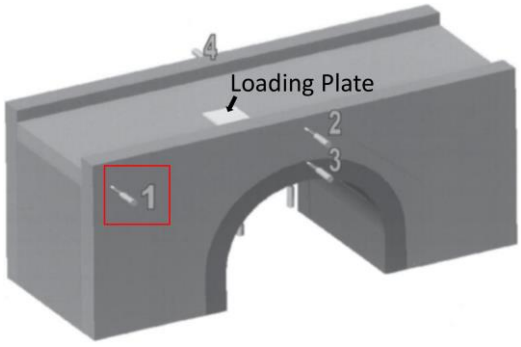

Figure 6. LVDT configuration and loading plate [10]

Both sides of the scaled bridge are confined with timber walls that are tied via steel cables. However, during the test, the end constraints are deflected through the span and transversal direction due to excessive soil pressure. This is confirmed in the numerical model and several different boundary conditions are tested to observe their influence on the capacity and deformability of the structure. Further discussion about the boundary conditions can be found next. It is worth noting that there is no sign of damage, i.e. hinge mechanism, or punching shear failure, observed at the arch barrel during the test. The governing collapse mechanism is recorded as spandrel wall failure.

There are four sets of load tests performed in the experiment. The highest peak load is measured in the first one, which is approximatelly 132 kN. At this load stage, the spandrel wall had reached the partial collapse state and external load was intentionally removed. Furthermore, vertical flexural cracks and detachment of arch barrel from spandrel wall were noticed at the end of the first test.

3.2 Numerical model

There are five different boundary conditions examined on the proposed discontinuum model (Figure 7).

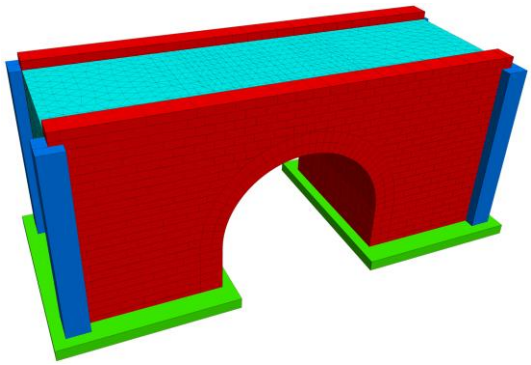

Figure 7. Mixed discrete-continuum model consisting of side supports, spandrel walls, arch barrel and backfill material

The translational degrees of freedom of the nodes located at both ends of the backfill material are restricted in the span (longitudinal) direction, however, left free in vertical and transverse

This is a pre-print version of an article published in **Pulatsu B., Erdogmus E. and Lourenço P.B. (2019) *Discrete-continuum approach to assess 3D failure modes of masonry arch bridges,* IABSE Symposium, March 27-29**.

directions. Different boundary configurations are set by considering fixed, free and flexible side supports. Additionally, cable elements to replicate steel ties (Figure 8) and longer spandrel walls with inclined supports at the sides (Figure 9) are also implemented to discuss the structural behaviour observed in the experiment. Inclined supports simulate the situation where a bridge only has condensed earth on the embankments instead of a full masonry spandrel wall. Live load is applied through a rigid plate incrementally. The contact and material properties are given in Table 3 and Table 4.

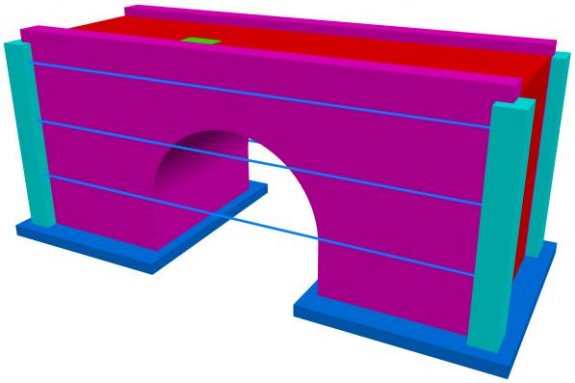

Figure 8. 3DEC model with cable elements

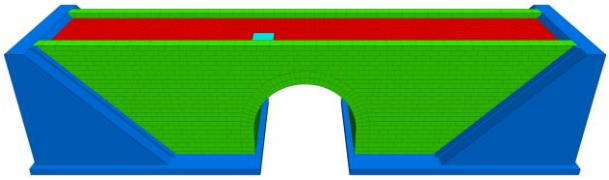

Figure 9. Model bridge with inclined spandrel walls

The results of the analysis for the various boundary conditions are given in Figure 10. As expected, the lack of confinement (free end constraints) yields the lowest capacity and pre-mature failure. On the other hand, fixed side supports provide extremely stiff model which does not reflect deflection at the end constraints occurred during the experiment. Inclined spandrel walls with rigid supports and elasto-plastic boundary conditions (i.e. flexible, steel ties) provide relatively close results to the experimental data (Figure 10).

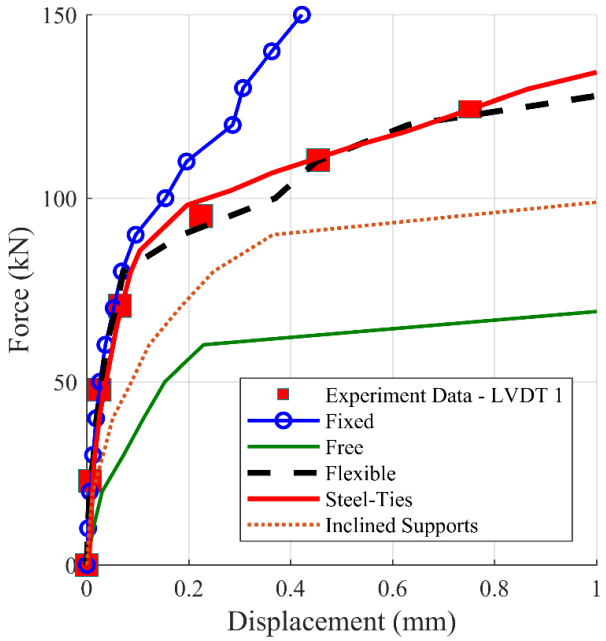

Figure 10. Force-Displacement curves of numerical model using different boundary conditions

Table 3. Contact properties at masonry.

Block Density [kg/m³]	k_n [Pa/m]	k_s [Pa/m]	ϕ [°]	c [Pa/m]
2500	80e+9	40e+9	37	0.45e+6
f_t [Pa/m]	ϕ_{res} [°]	c_{res} [Pa/m]		
0.30e+6	30	0.01e+6		

Table 4. Contact properties between masonry-soil

k_n [Pa/m]	k_s [Pa/m]	ϕ [°]	c [Pa/m]	f_t [Pa/m]
1e+9	1e+9	25	0	0

There are similar damage patterns and partial collapse mechanism observed in the numerical models compared to the experiment, for the intermediate response models. The first crack is noticed between spandrel wall and arch barrel, followed with a complete detachment through the end of the test. Then, flexural tensile cracks are observed on the spandrel wall close to the loading plate. Finally, a significant reduction of the stiffness and successive cracks at the joints are obtained, once the sliding of the spandrel wall over the arch barrel is captured under incremental vertical loads as shown in Figure 11.

This is a pre-print version of an article published in **Pulatsu B., Erdogmus E. and Lourenço P.B. (2019)** ***Discrete-continuum approach to assess 3D failure modes of masonry arch bridges,*** **IABSE Symposium, March 27-29**.

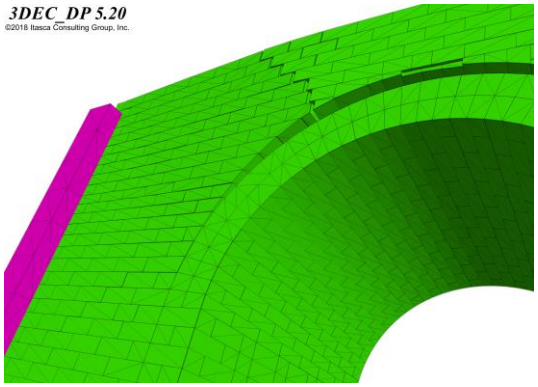

Figure 11. Shifting of spandrel wall and tensile cracks on the spandrel wall.

3.3 Influence of the frictional resistance between masonry-soil

The interaction between masonry and soil has a notable influence on the masonry arch bridges in terms of load bearing capacity and behaviour. Here, a parametric study is performed utilizing four different friction angles at the masonry-soil interface where there is no dilatancy considered. The discrete-continuum model with inclined spandrel wall is employed for the analysis since it represents the general masonry arch bridge state. Furthermore, the results are independent of the steel-ties and extra boundary condition parameters.

Results of the analysis indicated that lower interface friction angles lead lower load carrying capacity with higher deformation, as shown in Figure 12. It is worth noting that combined sliding and overturning failure mode is observed in all numerical models even for high friction angles. The failure mechanism is governed by the excessive deflection at the spandrel walls towards the out-of-plane direction. However, sliding phenomena may not necessarily be obtained during the collapse mechanism, depending on the depth of soil backfill, stiffness of the backfill, boundary conditions and height of spandrel wall, among others. Finally, when there is a lack of experimental tests to designate interface friction angle between masonry and soil, the practical solution of 2/3 of the soil backfill seems to provide appropriate safety margin for the analysis.

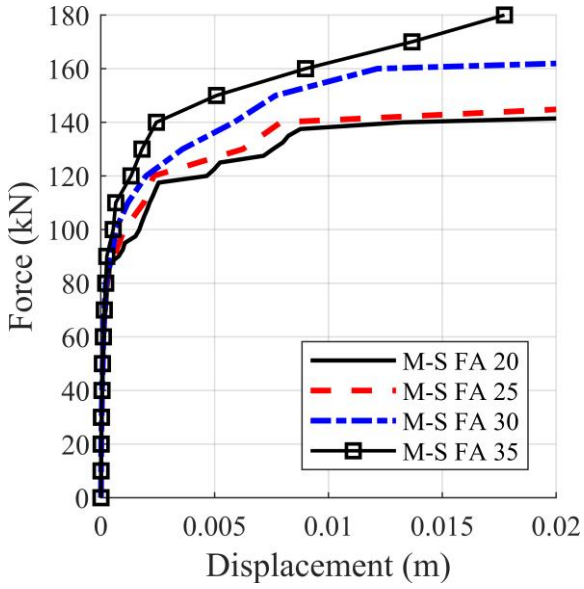

Figure 12. Force vs Displacement curves for different friction angle (FA) between masonry and soil (M-S)

4. Skew arches

Masonry arch bridges do not always span the distances perpendicularly but with an angle depending on the conditions at the site. Two most common construction techniques for skew masonry arch bridges are helicoidal skew and false skew, shown in Figure 13. In this research, the influence of these two construction methods on the behaviour and strength of the skew masonry arches are analysed under point and line load effects. The results of the analysis improve upon the findings of the recent study [14] and provide a deeper understanding of 3D structural behaviour of single and multi-ring skew masonry arches. It important to note that skew masonry arches reveal complex cracking mechanism and 3D flexural deflections that may be better simulated via discrete element approach. Again, rigid blocks are used to represent masonry units and Coulomb-slip joint model with tension cut-off is considered at the joints. Thus, crushing of masonry units are not taken into consideration. There are two experimental studies employed to validate discrete element models.

This is a pre-print version of an article published in **Pulatsu B., Erdogmus E. and Lourenço P.B. (2019)** ***Discrete-continuum approach to assess 3D failure modes of masonry arch bridges,*** **IABSE Symposium, March 27-29**.

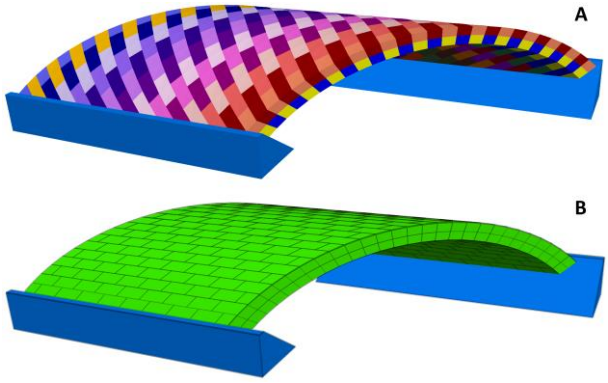

Figure 13. Construction techniques: Helicoidal method (A) and False skew (B)

First, a small-scale 45° skewed masonry arch barrel constructed by helicoidal method is analysed. It spans 1.2 meters with a span/rise ratio of 4. The masonry arch model is subjected to monotonically increasing forces applied at quarter-point (Figure 14). The material and contact parameters are given in Table 5.

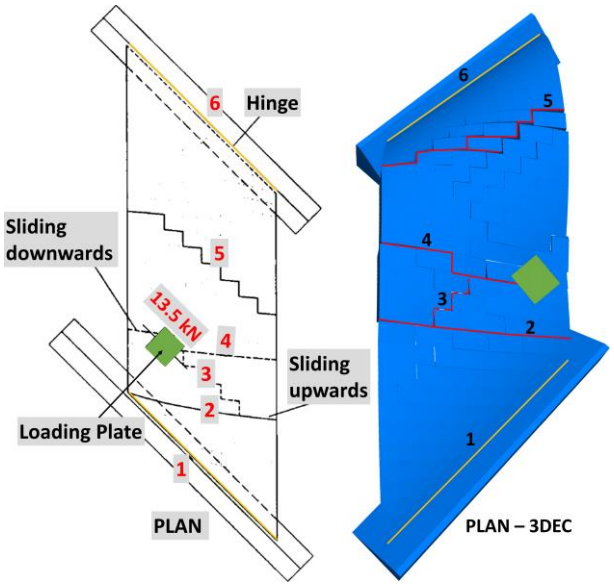

Figure 14. Damage state – Plan view (Left: Experiment [15], Right: Numerical model)

Table 5. Contact properties of discrete model

ρ [kg/m^3]	k_n [Pa/m]	k_s [Pa/m]	ϕ [°]	c [Pa/m]	f_t [Pa/m]
2400	80e+9	40e+9	35	100e+3	70e+3

In Figure 14, the obtained damage state along with the corresponding fracture pattern are shown at edge of collapse. The straight fracture lines, indicating plastic hinges (6 and 1), are observed at the supports, whereas, zig-zag types of cracks are captured on the arch barrel (5,4 and 3). Moreover, torsional rotation is noticed through the fracture line number 2, in which noticeable sliding between masonry units are also recorded. The flexural tensile cracks at the intrados and the sliding movement of the masonry blocks are shown in Figure 15. Hence, rather complex behaviour is observed exhibiting relative block movements with combined rotational and translational collapse mechanisms. When numerical results are compared to prior experimental results, a good agreement is achieved both qualitatively (comparison of crack patterns and locations) and quantitively. The load carrying capacity is found as 13.6 kN with less than 2% deviation from the experiment. Then, validated numerical model is further used to simulate the same arch geometry constructed with false skew method. In that case, simple hinging mechanism is obtained with much lower load carrying capacity, 6.72 kN.

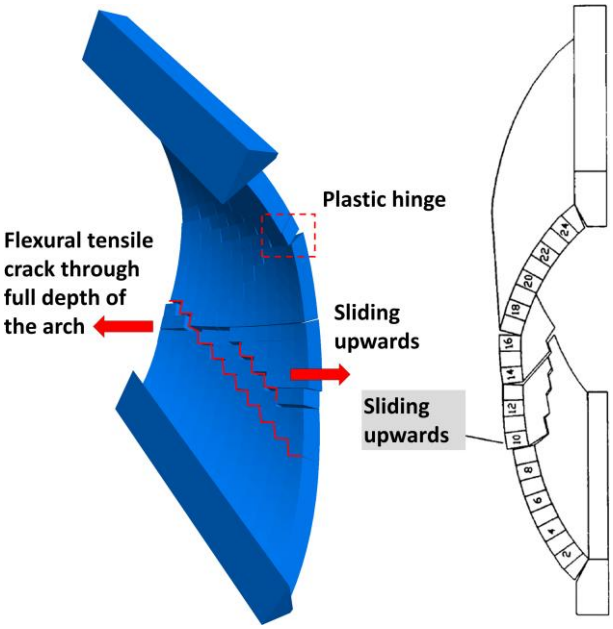

Figure 15. Damage state – Intrados (Right: Experiment [15], Left: Numerical model)

Secondly, the significant influence of construction method is further explored with another 45° skewed masonry arch barrel model, subjected to a

This is a pre-print version of an article published in **Pulatsu B., Erdogmus E. and Lourenço P.B. (2019)** ***Discrete-continuum approach to assess 3D failure modes of masonry arch bridges,*** **IABSE Symposium, March 27-29**.

line load applied at quarter span, as shown in Figure 16-A. The model bridge has 3 m clear span, constructed with helicoidal bond pattern and composed of two-layer with a total thickness of 0.22 m. Further details about the test setup can be found in [15]. The same elastic properties are used according to the previous arch barrel-only mode. However, the cohesion and tensile strength are taken as 0.5e+6 MPa/m and 0.35e+6 MPa/m, respectively.

The results of the analysis in terms of ultimate damage state is shown in Figure 16. There are two distinctive fracture patterns observed at the intrados and extrados. Furthermore, ring separation and sliding deformations of the masonry blocks are captured during loading (see Figure 16-A). Torsional rotation (twisting) and plastic hinging mechanisms are noted that are in lined with the experimental observations. The load carrying capacity of the numerical model, constructed with helicoidal method and experiment are given Table 6.

Furthermore, the same masonry arch model built up with false skew method is analysed. Again, there is a significant capacity (98 kN) reduction obtained for false skew arch with a simple hinging mechanism (Table 6).

Table 6. Load carrying capacity of 3 m span skew arch model constructed with helicoidal and false methods

Experiment [Helicoidal]	Discrete Model [Helicoidal]	Discrete Model [False Skew]
202	208	98

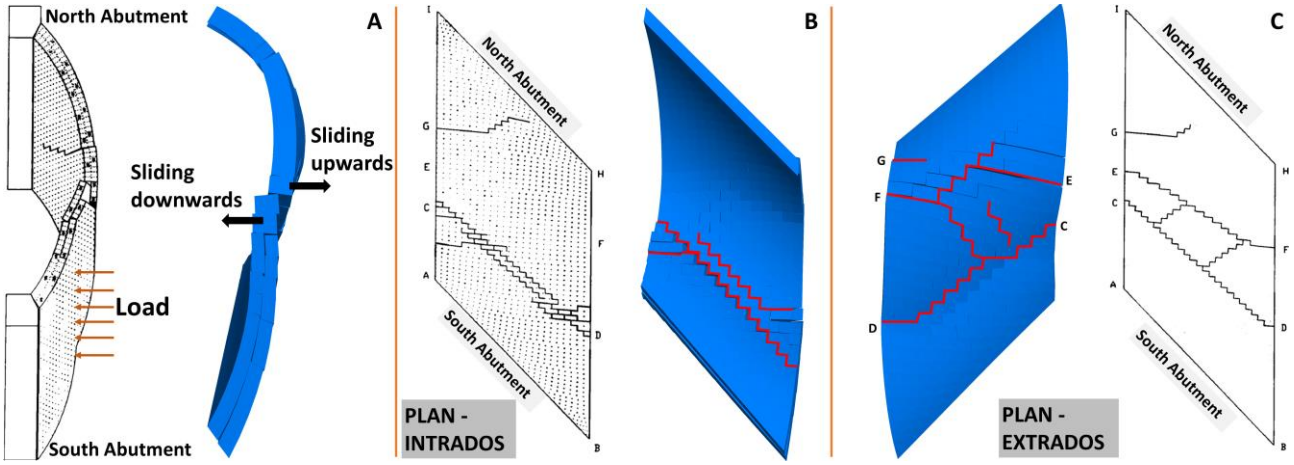

Figure 16. Double layer (3 m span) skew masonry arch barrel (Experimental and numerical damage states)

5. Conclusions

In this research, 3D collapse mechanisms of masonry arch structures are investigated by means of discrete and discrete-continuum approaches. Several experimental studies are utilized to validate the numerical models. The significant effect of boundary conditions on the strength and behaviour of spandrel walls are indicated by considering various boundary conditions. The out-of-plane failure mode of spandrel wall is successfully captured, which governs the capacity and serviceability of the bridge. Furthermore, positive effects of frictional interaction between soil backfill and masonry are highlighted via parametric analysis. Finally, skew arch barrels are investigated that are constructed with false and helicoidal methods. The results indicate the noticeable influence of helicoidal construction technique on the load carrying capacity and complex failure modes of skew masonry arches. The presented simulations demonstrate not only the potential of the employed numerical modelling strategy but also provide better understanding of 3D failure modes of the masonry arch structures.

This is a pre-print version of an article published in **Pulatsu B., Erdogmus E. and Lourenço P.B. (2019)** ***Discrete-continuum approach to assess 3D failure modes of masonry arch bridges,*** **IABSE Symposium, March 27-29**.

6. Acknowledgment

Authors would like to express their gratitude to Itasca Educational Partnership Program (IEP) for their kind support and providing 3DEC software. Furthermore, we would like to acknowledge the valuable help of Dr. Jim Hazzard, Itasca Consulting Group, and Dr. Jose Lemos, LNEC, Portugal, for their technical support.

7. References

[1] Citto C. and Woodman D. (2015). Evaluating existing and historical stone arch bridges. *STRUCTURE*, pp. 14-18.

[2] Melbourne C, Gilbert M. The behaviour of multiring brickwork arch bridges. *Structural Engineer*. 1995 Feb 7;73(3).

[3] Roca P, Molins C. Experiments on arch bridges. Arch Bridges IV-Advances in Assessment, Structural Design and Construction, P Roca & C Molins (Eds), Barcelona. 2004:365-74.

[4] Page J. Load tests to collapse on two arch bridges at Strathmashie and Barlae. 1989

[5] Pulatsu B, Erdogmus E, Bretas EM. Parametric study on masonry arches using 2D discrete element modelling. J Archit Eng. 2018; 24(2):1-9

[6] Toth AR, Orban Z, Bagi K. Discrete element analysis of a stone masonry arch. Mech Res Commun. 2009;36(4):469-80.

[7] Pulatsu B, Erdogmus E, Lourenco PB. Comparison of in-plane and out-of-plane failure modes of masonry arch bridges using discontinuum analysis. Eng Struct. 2019;178:24-36.

[8] Pulatsu B, Erdogmus E, Lourenco PB. Simulation of Masonry Arch Bridges Using 3D Discrete Element Modeling. In Structural Analysis of Historical Constructions 2019 (pp. 871-880). Springer, Cham.

[9] ITASCA. 3DEC – Universal distinct element code manual. Theory and background. Minneapolis: Itasca Consulting Group.

[10] Lourenço PB, Martins JP. Survey of old bridges over Rivers Ave and Vizela. In Arch'01. Eds. C. Abdunur, Presses Ponts et Chaussees 2001.

[11] Erdogmus E, Boothby T. Strength of spandrel walls in masonry arch bridges. Transport Research Record: Journal of the Transportation Research Board. 2004 Jan 1 (1892):47-55

[12] Boothby T., Yurianto Y, Erdogmus E. Experimental replication of masonry arch bridge spandrel wall collapse. The Masonry Society Journal. 2005; 23(1)

[13] Pulatsu B, Erdogmus E, Lourenço PB. Simulation of Masonry Arch Bridges Using 3D Discrete Element Modeling. In Structural Analysis of Historical Constructions 2019 (pp. 871-880). Springer, Cham.

[14] Forgács T, Sarhosis V, Bagi K. Influence of construction method on the load bearing capacity of skew masonry arches. Engineering Structures. 2018 Aug 1; 168:612-27.

[15] Hodgson JA. The behaviour of skewed masonry arch bridges (Doctoral dissertation, University of Salford).